ACS Sustainable Chemistry & Engineering

Research Article

Cite This: ACS Sustainable Chem. Eng. 2019, 7, 156−164

pubs.acs.org/journal/ascecg

Lithium-Ion Battery Anodes of Stacked Nanowire Laminate for Ultrahigh Areal Capacities

Wei-Chung Chang,[‖] Shih-Pin Lu,[‖] Hsun-Chen Chu, and Hsing-Yu Tuan*

Department of Chemical Engineering, National Tsing Hua University, 101, Section 2, Kuang-Fu Road, Hsinchu, Taiwan 30013, ROC

Supporting Information

ABSTRACT: Herein, a stacked Ge/Cu nanowire (NW) laminate made by stacking several Ge/Cu nanowire laminates accompanied by the conductive glue adhesives is used to achieve high capacity output per unit area (>10 mA h cm^{-2}). The combination of Cu NWs and conductive adhesives constructs a tough and conducting network through the electrode, and the stacked Ge/Cu nanowire laminate electrodes can load an ultrahigh mass of 14.8 mg Ge per unit area and provide an areal capacity output over 16 mA h cm^{-2}. A full-cell with an areal capacity of 11 mA h cm^{-2} built by stacked Ge/Cu nanowire laminate anode and $Li(Ni_{0.5}Co_{0.3}Mn_{0.2})O_2$ cathode was prepared and used to supply electricity for electronic devices, demonstrating their potential to be a candidate anode for high areal capacity Li-ion microbatteries that can be used for high-tech and integrated microsystems with limited space.

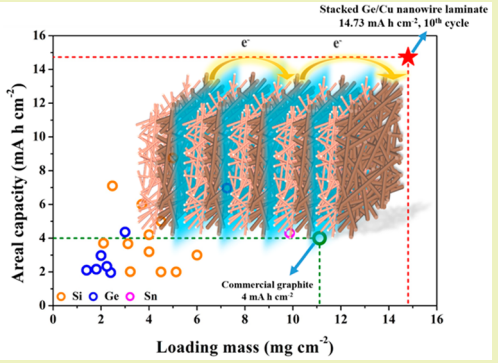

KEYWORDS: *Germanium, Nanowires, Ultrahigh areal capacity, Stacked laminate structure, Multilayered structure, Lithium-ion batteries, Anodes*

INTRODUCTION

Lithium-ion batteries (LIBs) are the most ideal energy storage systems for electronic applications, including portable devices, electric vehicles, and large stationary powering stations, owing to their long-term cycling life and high energy density.[1,2] Recently, to meet the ever-growing demands of energy density, intense research focused on developing high theoretical capacity anode materials. In spite of the substantial progress in cycle stability, most of the research concentrated on the improvement of the specific value calculated on the basis of the mass of the active materials but did not evaluate their performance in a high areal mass loading. Only a few reports show areal capacities that can have around the same level of commercial graphite anodes (3−4 mA h cm^{-2}).[3−8] In fact, the emerging smart microsystems require lithium-ion microbatteries (LIMBs) possessing the high energy and the power output per unit area.

There are two effective strategies to construct an ideal anode with high areal capacity: (i) Using high-theoretical specific capacity materials (>1000 mA h g^{-1}) such as Si (3579 mA h g^{-1}), P (2596 mA h g^{-1}), Ge (1384 mA h g^{-1}), and Sn (994 mA h g^{-1})[9−11] instead of the commercial graphite (372 mA h g^{-1}) as anodes can significantly increase the capacity output per unit area based on the same mass and thickness.[9−11] Although bulk high-capacity anode materials pulverize due to the enormous volume change (>300%) during lithiation/delithiation processes, diverse nanostructurization of high capacity materials has been developed to address the volume expansion issues and extend battery cycle life.[12−21] (ii) Building a network architecture through the electrode by selecting adaptable conducting materials such as carbon nanotubes (CNTs), carbon nanofibers (CNFs), graphene, and metal nanowires (NWs) can facilitate the transportation of electrons and enhance the electrochemical performance of electrodes. For example, Zhang et al. embedded the Si nanoparticles into a carbon framework, achieving an areal capacity of 3.7 mA h cm^{-2}.[22] Tian et al. fabricated a three-dimensional Ni−Sn NW network electrode, which can load an active materials mass loading of 9.86 mg cm^{-2}, delivering an areal capacity of 4.3 mA h cm^{-2}.[23]

Herein, we report a stacked nanowire laminate anode by stacking Ge/Cu nanowire laminates via the conducting glue adhesives composed of 3D cross-linked c-PAA-CMC and carbon black to achieve practical ultrahigh areal capacity (>10 mA h cm^{-2}) in LIBs. Stacked nanowire laminate allows ultrahigh Ge mass loading up to 14.8 mg cm^{-2}, which corresponds to an areal capacity of 19.5 mA h cm^{-2} (1st lithiation process) and a reversible areal capacity of 16 mA h cm^{-2} (5th lithiation process). This result indicates that the design of the stacked nanowire laminate structure can achieve nearly complete lithiation of active materials in thick and high mass loading electrode. As a proof-of-concept, a coin full-cell built by a stacked Ge/Cu nanowire laminate anode and a $Li(Ni_{0.5}Co_{0.3}Mn_{0.2})$ cathode with an areal capacity of 11 mA h

Received: May 25, 2018
Revised: September 27, 2018
Published: November 13, 2018

DOI: 10.1021/acssuschemeng.8b02409
ACS Sustainable Chem. Eng. 2019, 7, 156−164

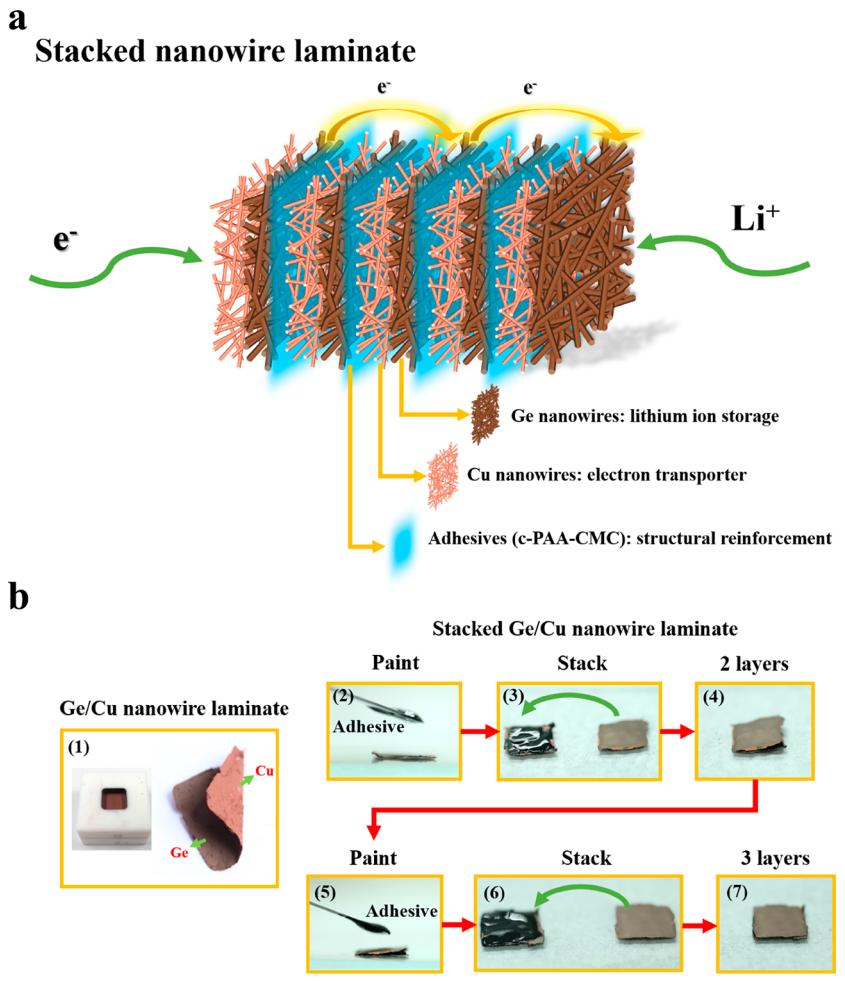

Figure 1. (a) Schematic design of stacked nanowire laminate electrodes. (b) Fabrication process of the stacked Ge/Cu nanowire laminate electrode.

cm^{-2} was prepared to demonstrate their potential uses on microrechargeable Li-ion battery anodes with ultrahigh capacity output per unit area.

RESULTS AND DISCUSSION

Stacked Ge/Cu nanowire laminate electrodes were fabricated by assembling several Ge/Cu nanowire laminates via the conductive glue composed of 3D cross-linked poly(acrylic acid)-carboxymethycelluose sodium salt (c-PAA-CMC) and carbon black. Figure 1a shows the schematic representation of the stacked Ge/Cu nanowire laminate electrode comprised of three tightly tangled Ge/Cu laminates and adhesives sandwiched between each laminate. Detailed analysis including the SEM and TEM images and XRD patterns of Ge NWs and Cu NWs was shown in Figure S1. The diameter and length of a Ge NW is around 30−50 nm and over 100 μm, respectively. The XRD pattern recorded from Ge NWs shows five apparent peaks between 20° and 80°, being consistent with the typical characteristic (111), (220), (311), (400), and (331) reflection of crystalline Ge. The size of a Cu NW is 50−100 nm in diameter, and its length is around 50 μm. In the XRD pattern of Cu NWs, there are three peaks located at around 43.5°, 50.8°, and 74.5°, corresponding to the (111), (200), and (220) reflection of crystalline Cu. As shown in Figure 1b, a Ge/Cu nanowire laminate was prepared by dropping the dispersion of Cu NWs in toluene onto the polytetrafluoroethylene (PTFE) mold followed by dropping the dispersion of Ge NWs in toluene onto the completely dried Cu NWs (first image of Figure 1b). Then, the conductive adhesives composed of the PAA-CMC and the carbon black were painted onto the surface of Ge/Cu nanowire laminate, as shown in the second image of Figure 1b. Next, a stacked Ge/Cu nanowire laminate structure was formed by stacking another Ge/Cu nanowire laminate up against the adhesives, as shown in the third and fourth image of Figure 1b. A higher areal capacity electrode can be obtained by repeating the step of painting the conductive adhesives and stacking the Ge/Cu nanowire laminates (fifth to seventh image of Figure 1b). Each Ge/Cu nanowire laminate was composed of approximately 3 to 4 mg of Ge NWs and 1 mg of Cu NWs. The proportion of the Ge NWs is 75−80% in each laminate. Detailed values of the thicknesses of the Ge NWs, Cu NWs, and conductive adhesive layers are shown in the Table S1. The stacked Ge/Cu nanowire laminate electrodes were heated at 150 °C for 2 h to induce the condensation reaction between the PAA and CMC to form cross-linked PAA-CMC (c-PAA-CMC), making the stacked Ge/Cu nanowire laminate electrode tougher to accommodate the volume expansion during cycling tests. Figure 2a shows the cross-sectional SEM images of a stacked Ge/Cu nanowire laminate electrode. Figure 2b−e shows the EDS mapping of stacked Ge/Cu nanowire laminate electrode: the red dots, green dots, and blue dots correspond to the Cu NWs, Ge NWs, and conductive

DOI: 10.1021/acssuschemeng.8b02409
ACS Sustainable Chem. Eng. 2019, 7, 156−164

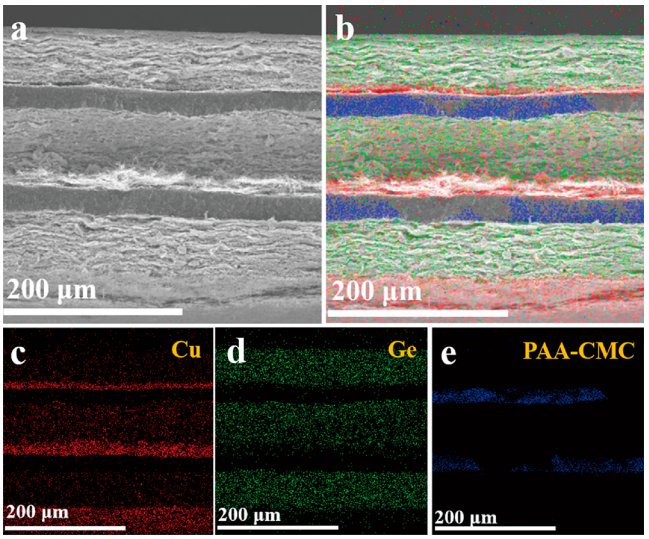

Figure 2. (a) Cross-sectional SEM images of stacked Ge/Cu nanowire laminate electrode composed of three Ge/Cu laminates. (b) EDS mapping corresponding to (a). The corresponding EDS profile for (c) Cu, (d) Ge, and (e) c-PAA-CMC adhesive.

adhesives, respectively. Notably, the thickness observed from the cross-sectional SEM image is not accurate and different from the values of Table S1 measured by the thickness gauge. This issue could be attributed to two possible causes: (1) The tilt angle is not adequate; thus, some surface areas included in the cross-sectional SEM image result in a higher thickness value. (2) The cross section of stacked nanowire laminate is not uniform; the NWs might overlap to other layer, leading to an imprecise thickness.

The electrochemical performance of Ge/Cu laminate electrode was evaluated by using galvanostatic discharge/charge measurements between the voltage of 0.01 and 1.5 V in the CR2032 half-cells (1 C = 1000 mA h g^{-1}). Figure 3a shows the electrochemical performance of a single Ge/Cu laminate electrode and a stacked Ge/Cu nanowire laminate electrode containing 8.8 and 8.5 mg of Ge NWs at the rate of 0.1 C, respectively. Their corresponding specific capacity and Coulombic efficiency were shown in Figure S2. A single Ge/Cu laminate electrode loaded with 8.8 mg of Ge NWs exhibited high areal capacity of 10.5 mA h cm^{-2} in the first cycle and maintained the reversible areal capacity over 9 mA h cm^{-2} after 10 cycles. However, rapid capacity fade occurred after 15 cycles, and the reversible capacity remained only 1.7 mA h cm^{-2} in the 30th cycle. Three layers of stacked Ge/Cu nanowire laminate loaded with 8.5 mg of Ge NWs showed an areal capacity of 11.5 mA h cm^{-2} in the first cycle and maintained the reversible areal capacity of 8.5 mA h cm^{-1} in

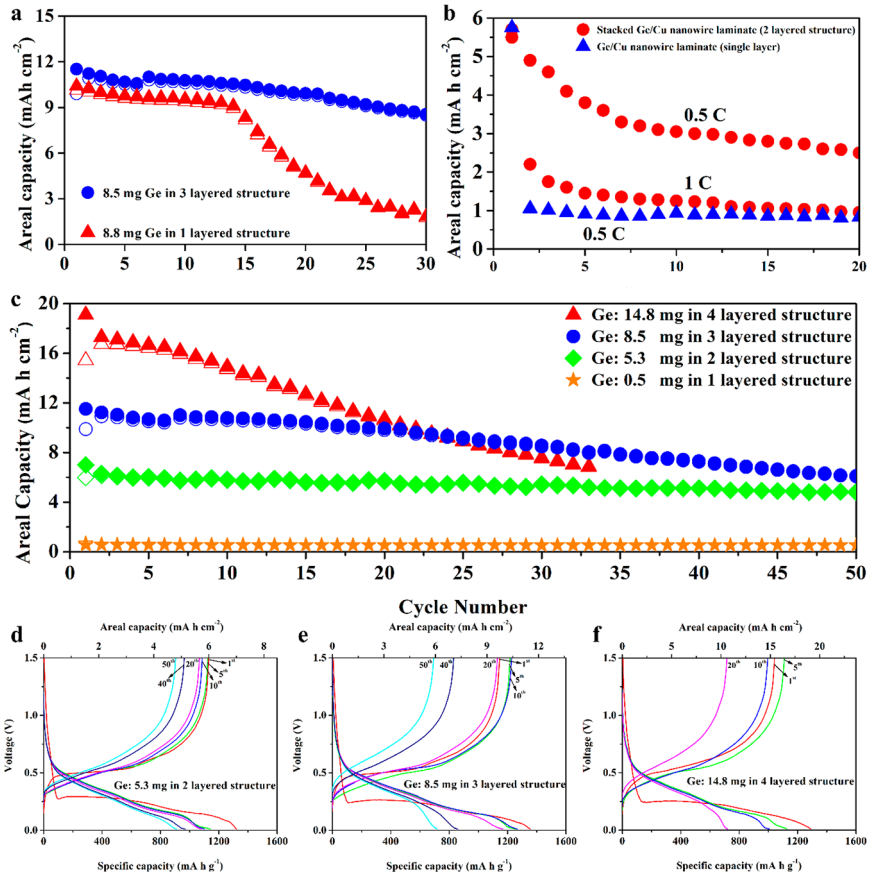

Figure 3. (a) The electrochemical performance of the a single Ge/Cu laminate electrode with the Ge mass loading of 8.8 mg cm^{-2} and the stacked Ge/Cu nanowire laminate electrode with the Ge mass loading of 8.3 mg cm^{-2}. Both electrodes were operated at the rate of 0.1 C. (b) Stacked Ge/Cu nanowire laminate (2 layered structure) cycled at the rate of 0.5 and 1 C (red dots). Ge/Cu nanowire laminate (single layer) cycled at the rate of 0.5 C (blue triangles). (c) Cycling performance of the stacked Ge/Cu nanowire laminate electrode with different Ge mass loading of 0.5 mg (1 layer), 5.3 mg (2 layers), 8.5 mg (3 layers), and 14.8 mg (4 layers) at the rate of 0.1 C. (d–f) Voltage profile corresponding to 2 layered structure, 3 layered structure, and 4 layered structure of (c), respectively.

DOI: 10.1021/acssuschemeng.8b02409
ACS Sustainable Chem. Eng. 2019, 7, 156−164

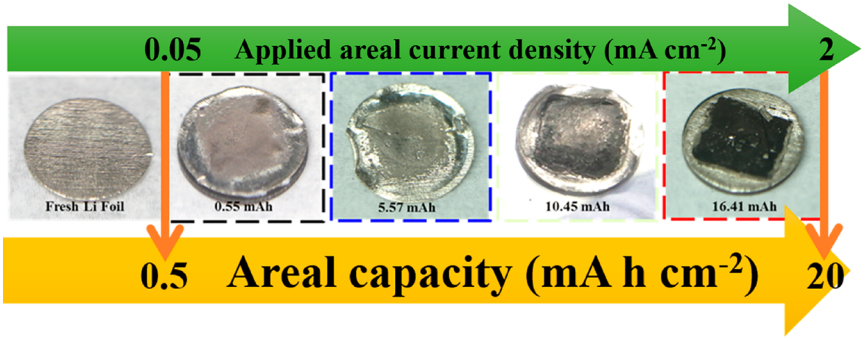

Figure 4. Images of the Li foil before the half-cell evaluation and after 10 electrochemical cycles. The five images, from left to right, show original Li foil and Li foil cycled at an areal capacity of 0.55, 5.57, 10.45, and 16.41 mA h cm^{-2} at the rate of 0.1 C.

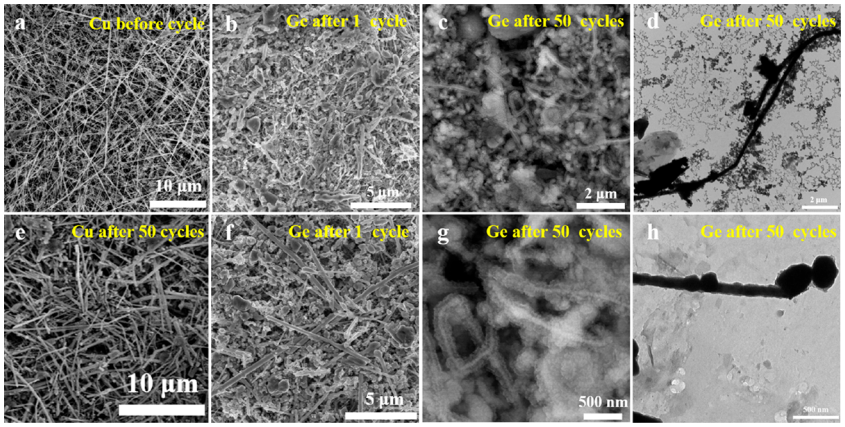

Figure 5. (a) SEM image of Cu NWs before cycle. (b, f) SEM images of Ge NWs after 1 cycle. (c, g) SEM images of Ge NWs after 50 cycles. (d, h) TEM images of Ge NWs after 50 cycles. (e) SEM images of Cu NWs after 50 cycles.

the 30th cycle, corresponding to an 81% retention capacity with respect to the fifth cycle. This result revealed that the cycling performance was significantly improved by the stacked laminate structure. Additionally, the performances of stacked Ge/Cu nanowire laminate electrodes (2 layered structure) cycled at 0.5 and 1 C were shown in Figure 3b. Compared to the single layered Ge/Cu nanowire laminate, which only delivers a low areal capacity (~1 mA h cm^{-2}) at the rate of 0.5 C, the rate capability was apparently improved by using the stacked nanowire laminate structure.

The cycling performance of the stacked Ge/Cu nanowire laminate electrodes with the Ge mass loading of 0.5 mg (1 layer), 5.3 mg (2 layers), 8.5 mg (3 layers), and 14.8 mg (4 layers) was evaluated at the rate of 0.1 C, as shown in Figure 3c. The corresponding specific capacity and Coulombic efficiency were shown in Figure S3. The 1 layered, 2 layered, 3 layered, and 4 layered Ge/Cu electrodes delivered initial discharge areal capacities of 0.67, 7.00, 11.51, and 19.09 mA h cm^{-2}, corresponding to the specific capacities of 1340, 1321, 1354, and 1289 mA h g^{-1}, respectively. Figure S4 depicts that the increase in areal capacity is directly proportional to the rise of Ge mass loading. The results showed the high utilization of Ge of 95.6% (2 layers), 97.8% (3 layers), and 93.1% (4 layers) according to its theoretical specific capacity of 1384 mA h g^{-1}, revealing that the Ge could be nearly completely converted to the Li germanide ($Li_{3.75}Ge$) in the stacked nanowire laminate structures even at ultrahigh mass loading of Ge of 14.8 mg. In the first charge process, stacked Ge/Cu nanowire laminate electrodes showed reversible areal capacities of 5.99 (2 layers), 9.88 (3 layers), and 15.41 (4 layers) mA h cm^{-2}, corresponding to the Coulombic efficiencies of 85.6%, 85.8%, and 80.1%, respectively. Figure 3d–f shows the voltage profile corresponding to Figure 3c. The first cycle that corresponds to the lithiation of crystalline Ge (~0.25 V)[24] is different from the other cycles; in the second cycle, the curves contributed by the lithiation of amorphous Ge were consistent with the previous literature.[15,16,25] A small plateau appeared at near 0 V that was an occurrence of lithium plating[26] on the surface of stacked Ge/Cu nanowire laminate electrode. In the following cycles, the Coulombic efficiencies of all the stacked Ge/Cu nanowire laminate electrodes were over 99%. After 10 cycles, stacked Ge/Cu nanowire laminate electrodes exhibited the reversible areal capacities of 5.76 (2 layers), 10.61 (3 layers), and 14.73 (4 layers) mA h cm^{-2}, corresponding to the retention of 96.6%, 100.1%, and 89.8% (with respect to the fifth cycle), respectively. The electrochemical performance of stacked Ge/Cu nanowire laminate electrodes significantly overpasses the pure Ge nanowire laminate (the areal Ge mass loading was ~0.5 mg), which only delivers 838 mA h g^{-1} and the retention of 88.9% after 10 cycles, as shown in Figure S5. These results further demonstrate that the design of stacked Ge/Cu nanowire laminate is an efficient structure for the transportation of Li-ions and electrons in the thick and high mass loading electrodes. As a result, the stacked Ge/Cu nanowire laminate comprised of 2 layered Ge/Cu laminate showed stable cycle performance, maintaining an areal capacity of around 5 mA h cm^{-2} that corresponds to the retention of 83% after 50 cycles, whereas in the 3 and 4 layered laminate electrodes the rapid capacity fade occurred after 20 and 7 cycles, respectively. The evaluated halfcells with ultrahigh Ge

DOI: 10.1021/acssuschemeng.8b02409
ACS Sustainable Chem. Eng. 2019, 7, 156–164

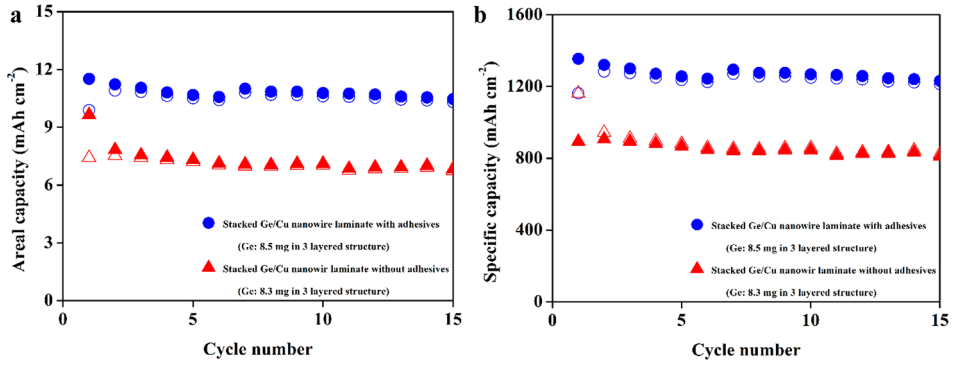

Figure 6. (a) Areal capacity of stacked Ge/Cu nanowire laminate with/without adhesives at the rate of 0.1 C. (b) Specific capacity of stacked Ge/Cu nanowire laminate with/without adhesives at the rate of 0.1 C.

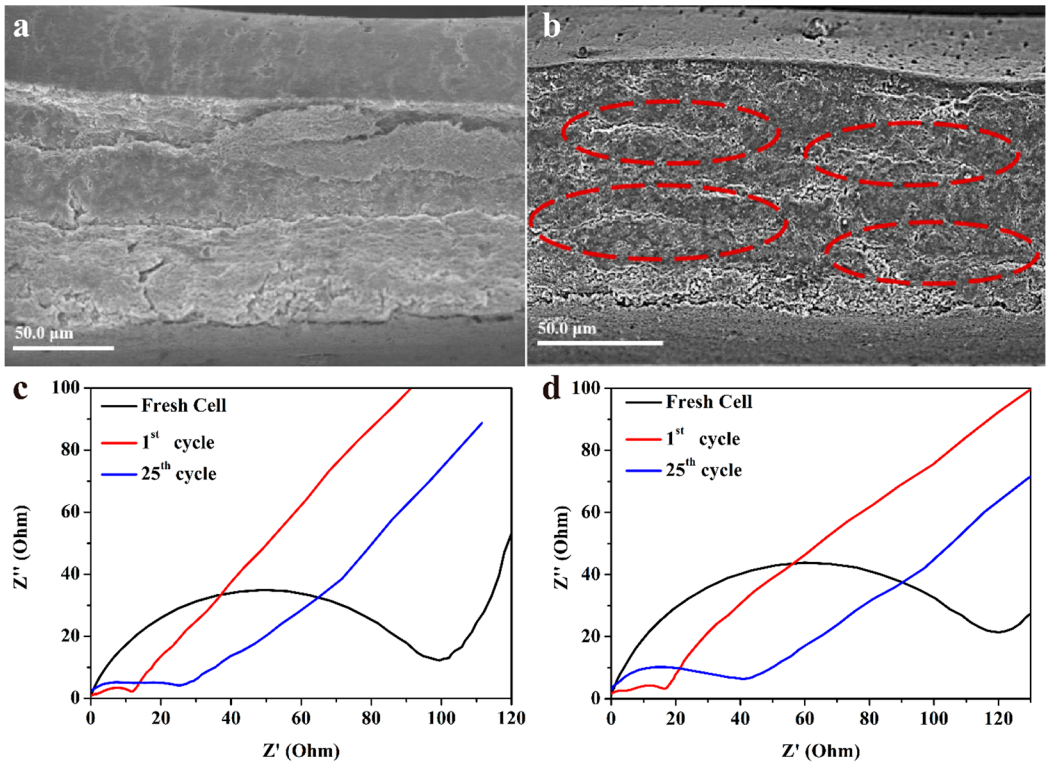

Figure 7. (a) Cross-sectional SEM image of stacked Ge/Cu nanowire laminate electrode after 25 cycles. (b) Cross-sectional SEM image of single Ge/Cu nanowire laminate electrode after 25 cycles. (c) Nyquist plots of the stacked Ge/Cu nanowire laminate electrode half-cell before cycle and after various cycles: 1st and 25th. (d) Nyquist plots of the single Ge/Cu nanowire laminate electrode half-cell before cycle and after various cycles: 1st and 25th.

mass loading started to fail owing to the counter electrodes of Li metal, which became fractured and have large amounts of mossy and dendritic Li growth, as shown in Figure 4. With higher current density, the growth of dendrites as well as the formation of the dead Li (the dendrites lost contact from the Li metal substrate) will be accelerated, leading to the continuous capacity fading.[27−30]

Stacked nanowire laminate structure enables ultrahigh reversible areal capacity (>15 mA h cm^{-2}) per unit area. This structure built by NWs possesses lots of voids that make the electrode able to be easily wetted by the electrolyte. Cu NWs penetrate between the layers of Ge and build interconnecting networks to accelerate the electron transport as well as grasp the adjacent Ge NWs to accommodate the expansion/contraction during the lithiation/delithiation process.[31−33] Furthermore, Cu NWs, which do not react with Li-ions, could form an intact layer to support fractured Ge after several cycles. As shown in Figure 5, most of the Ge NWs were fractured after 50 cycles, whereas Cu NWs retained their original morphology. Conductive adhesives can make the whole electrode structure more compact, form a tough architecture, and further enhance the accommodation capability of the stacked nanowire laminate structure. Moreover, conductive adhesives filled into the interspace of Cu NWs and Ge NWs can prevent the formation of Cu_3Ge. To form a stacked Ge/Cu nanowire laminate without conductive adhesives, the solution of Ge NWs and Cu NWs needs to be repeatedly placed into the PTFE mold. After a 500 °C heat treatment, Cu_3Ge was found to form in the structure of adhesive-free stacked Ge/Cu nanowire laminate (see the XRD pattern in Figure S6). The inactive property of Cu_3Ge to the Li-ions will lead to the decrease in the specific capacity.[34]

DOI: 10.1021/acssuschemeng.8b02409
ACS Sustainable Chem. Eng. 2019, 7, 156−164

Figure 6a,b shows the cycling performance of multilayered Ge/Cu with and without conductive adhesives. As a result, the adhesive-free stacked Ge/Cu nanowire laminate electrode only delivered a specific discharge/charge capacity of 1161/894 mA h g^{-1}, indicating that the formation of inert Cu_3Ge caused the reduction of specific capacity. Comparatively, the specific discharge/charge capacity of the stacked Ge/Cu nanowire laminate filled with conductive adhesives exhibited a high specific discharge/charge capacity of 1354/1162 mA h g^{-1}, showing higher utilization of Ge NWs. As shown in Figure 7a,b, under the near mass loading of the active materials, the cross-sectional SEM images revealed that the stacked nanowire laminate structure was still intact after 25 cycles, whereas a large number of horizontal cracks occurred in the single Ge/Cu laminate electrode. Figure 7c,d shows the electrochemical impedance spectroscopy (EIS) of the single Ge/Cu laminate electrode and the stacked Ge/Cu nanowire laminate electrode, respectively. Evidently, stacked Ge/Cu nanowire laminate showed lower resistance after 25 cycles via the addition of Cu NWs and conductive adhesives between Ge layers. Figure 8 presents the plots of the areal capacity against the active materials areal mass loading (the detailed data is shown in Table S2). These plots display the recent studies of alloy anode materials (data taken from refs 3, 5, 7, 14, 17, 22, 23, and 35−48), which achieve or overpass the areal mass loading level of commercial graphite, indicating that the stacked Ge/Cu nanowire laminate electrode reaches a new level of areal mass loading of 14.8 mg cm^{-2}, being 1.5 times higher than that of the second place. Moreover, stacked Ge/Cu nanowire laminate electrode with 14.8 mg cm^{-2} provided a reversible capacity of 16 mA h per unit area that utilized Ge of approximately 80%, ranking first place among all of the alloy anodes reported in the literature.

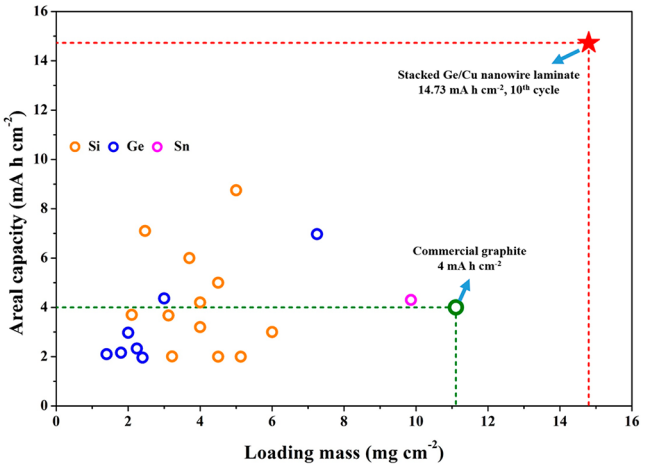

Figure 8. Comparison of stacked Ge/Cu nanowire laminate electrode and reported Ge, Si, Sn anodes at the rate of around 0.1 C. Data taken from refs 3, 5, 7, 14, 17, 22, 23, and 35−48. The detailed data is shown in Table S1.

To further solve the problems of the Li dendrite and demonstrate the viability of the stacked Ge/Cu nanowire laminate as an LIB anode, the coin fullcell comprising a stacked Ge/Cu nanowire laminate anode and a $Li(Ni_{0.5}Co_{0.3}Mn_{0.2})O_2$ cathode with an areal capacity of 11 mA h cm^{-2} was prepared (the electrochemical performance of $Li(Ni_{0.5}Co_{0.3}Mn_{0.2})O_2$ halfcell is shown in Figure S7). To avoid the occurrence of the Li plating on the anode, the areal capacity of the anode was around a 10% excess of that of the cathode, calculated on the basis of their first discharge specific capacity measured in the halfcell system. The fullcell was evaluated under the cutoff voltage ranging from 2.8 to 4 V, as shown in the Figure 9a,b. At the first charge process, the stacked Ge/Cu nanowire laminate anode in full-cell showed an areal charge capacity of 11.5 mA h cm^{-2}, corresponding to a specific capacity of 1350 mA h g^{-1}, which is near the theoretical specific capacity of Ge. This result indicates that the large amount of the Ge could achieve full lithiation in the stacked Ge/Cu nanowire laminate structure. At the first discharge process, stacked Ge/Cu nanowire laminate full-cell delivered an areal reversible capacity of 8.3 mA h cm^{-2}, corresponding to the Coulombic efficiency of 72.1%. In the following cycles, the Coulombic efficiency was increased to 99% gradually. After 50 cycles, the stacked Ge/Cu nanowire laminate full-cell still maintained an areal discharge capacity of 6.1 mA h cm^{-2} at a current density of 1.08 mA cm^{-2}. As mentioned previously, increased areal capacity accelerates the growth of Li dendrite and leads to the rapidly continuous capacity fade. The use of the NCM electrode instead of the Li metal foil can address the issue of the dendritic Li growth. As shown in Figure 9c, while the areal capacity was increased to over 8 mA h cm^{-2}, the retention of the stacked Ge/Cu nanowire laminate full-cell was over 75% after 50 cycles, which was apparently better than that of the half-cell (the retention of the half-cell was only 57% after 50 cycles). It is the first time that a Li-ion fullcell composed of an alloy anode achieved an ultrahigh areal capacity of over 10 mA h cm^{-2}. To further demonstrate the stacked Ge/Cu nanowire laminate fullcell availably work for a practical application, we prepared a stacked Ge/Cu nanowire laminate full-cell with an areal capacity of 11 mA h cm^{-1} (Figure 10a−c). This full-cell could drive a fan and 48 blue light emitting diodes (LEDs) that require 60 and 20 mA, respectively. Moreover, the stacked Ge/Cu nanowire laminate fullcell could light up 87 green LEDs and maintain the brightness of LEDs for more than 300 min, which is 3 times as high as that of the commercial graphite with 4 mA h cm^{-2}.

CONCLUSION

In conclusion, stacked Ge/Cu nanowire laminate anodes could provide ultrahigh capacity output per unit area. Using some Cu NWs as an intact layer that penetrates through the layers of Ge, building conductive channel networks to accelerate the transportation of electrons, and grasping the adjacent Ge NWs to accommodate the volume change in thick and high mass loading electrodes are necessary steps. Moreover, Cu NWs could support fractured Ge after several electrochemical cycles. Conductive adhesives composed of c-PAA-CMC and carbon black were filled between the Ge NWs and Cu NWs, thus making the structure of stacked Ge/Cu nanowire laminate electrodes become tougher and more compact, which further promotes the accommodation capability. Besides, conductive adhesives could prevent the formation of Cu_3Ge, reducing the impact of a decrease in capacity. With this optimal design, the areal capacity can directly increase proportionally to the rise of active materials mass loading. Stacked Ge/Cu nanowire laminate anodes showed high reversible areal capacities of around 6 mA h (2 layers) and 10 mA h (3 layers) and achieved an unreported ultrahigh mass loading of 14.8 mg Ge per unit area (4 layers) that can output a reversible areal capacity of over 16 mA h cm^{-2}, corresponding to the high utilization of Ge of 80%. Additionally, compared to the single layered Ge/Cu

DOI: 10.1021/acssuschemeng.8b02409
ACS Sustainable Chem. Eng. 2019, 7, 156−164

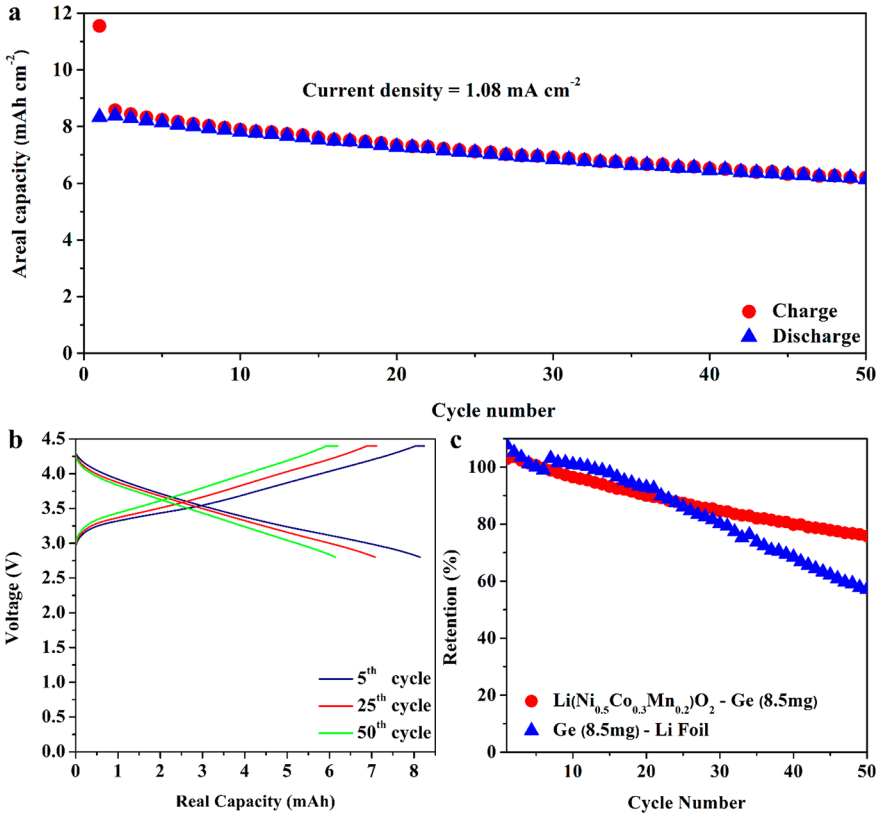

Figure 9. (a) Cycling performance of full-cell composed of stacked Ge/Cu nanowire laminate anode and commercial $Li(Ni_{0.5}Co_{0.3}Mn_{0.2})O_2$ cathode at the current density of 1.08 mA cm^{-2}. (b) Voltage profile corresponding to (a). (c) Retention with respect to the 5th cycle. The red dots correspond to the full-cell comprised of $Li(Ni_{0.5}Co_{0.3}Mn_{0.2})O_2$ cathode and stacked Ge/Cu nanowire laminate anode. The blue triangles correspond to the half-cell comprised of stacked Ge/Cu nanowire laminate cathode and Li foil anode.

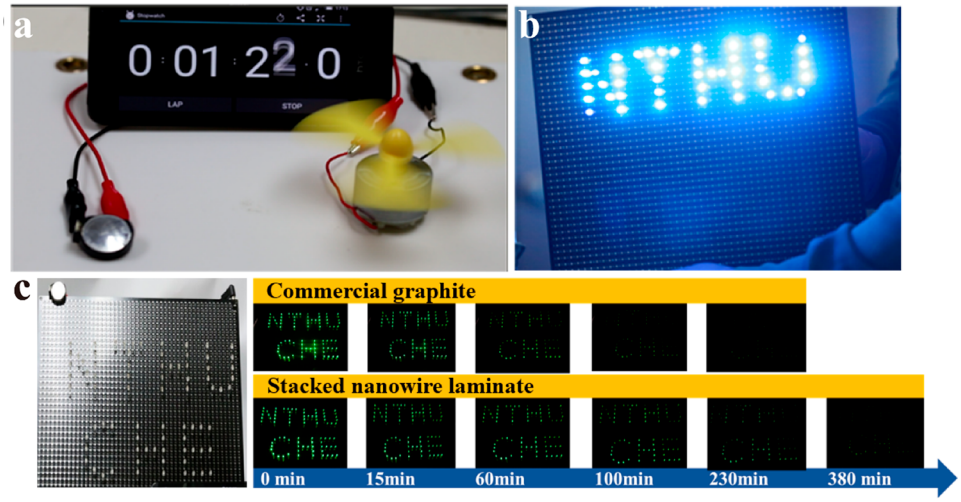

Figure 10. A coin full-cell composed of stacked Ge/Cu nanowire laminate anode with an areal capacity of 11 mA h cm^{-2} that could drive (a) a fan, (b) 48 blue LEDs, and (c) 83 green LEDs over 300 min.

nanowire laminate, the rate capability is significantly improved by the stacked nanowire laminate structure. Furthermore, an 11 mA h cm^{-2} fullcell composed of stacked Ge/Cu nanowire laminate as anode was prepared to show the viability of stacked Ge/Cu nanowire laminate as a LIB anode. Consequently, the design of stacked nanowire laminate structure provides a facile approach to fabricate ultrahigh areal capacity anodes. This concept may be an effective strategy to develop high areal capacity electrodes of other materials that are suitable for integrated microsystems with very limited space.

■ ASSOCIATED CONTENT

Supporting Information

The Supporting Information is available free of charge on the ACS Publications website at DOI: 10.1021/acssuschemeng.8b02409.

DOI: 10.1021/acssuschemeng.8b02409
ACS Sustainable Chem. Eng. 2019, 7, 156−164

Materials; Ge NWs synthesis and passivation; Cu NWs synthesis; fabrication of c-PAA-CMC adhesive slurry, Ge/Cu nanowire laminate, stacked Ge/Cu nanowire laminate electrode, and high areal capacity cathode; lithium-ion battery assembly and electrochemical characterization; characterization of Ge NWs; specific capacity and Coulombic efficiency; plot of the areal Ge mass loading against the areal capacity; cycling performance; XRD pattern; electrochemical performance; detailed values of thickness; detailed data of Figure 3 (PDF)

AUTHOR INFORMATION

Corresponding Author

*E-mail: hytuan@che.nthu.edu.tw.

ORCID

Hsing-Yu Tuan: 0000-0003-2819-2270

Author Contributions

‖W.-C.C. and S.-P.L. contributed equally to this work.

Notes

The authors declare no competing financial interest.

ACKNOWLEDGMENTS

The authors acknowledge the financial support by the Ministry of Science and Technology through the grants of NSC 102-2221-E-007-023-MY3, MOST 103-2221-E-007-089-MY3, MOST 103-2622-E-007-025, MOST 102-2633-M-007-002, and MOST 106-2628-E-007-005-MY3.

REFERENCES

(1) Janek, J.; Zeier, W. G. A solid future for battery development. *Nat. Energy* **2016**, *1*, 16141.

(2) Choi, J. W.; Aurbach, D. Promise and reality of post-lithium-ion batteries with high energy densities. *Nature Reviews Materials* **2016**, *1*, 16013.

(3) Lee, G.-H.; Lee, S.; Lee, C. W.; Choi, C.; Kim, D.-W. Stable high-areal-capacity nanoarchitectured germanium anodes on three-dimensional current collectors for Li ion microbatteries. *J. Mater. Chem. A* **2016**, *4*, 1060−1067.

(4) Chen, Z.; Wang, C.; Lopez, J.; Lu, Z.; Cui, Y.; Bao, Z. High-Areal-Capacity Silicon Electrodes with Low-Cost Silicon Particles Based on Spatial Control of Self-Healing Binder. *Adv. Energy Mater.* **2015**, *5*, 1401826.

(5) Chang, W.-C.; Kao, T.-L.; Lin, Y.; Tuan, H.-Y. Flexible All Inorganic Nanowire Bilayer Mesh as a High-Performance Lithium-Ion Battery Anode. *J. Mater. Chem. A* **2017**, *5*, 22662−22671.

(6) Forney, M. W.; Dzara, M. J.; Doucett, A. L.; Ganter, M. J.; Staub, J. W.; Ridgley, R. D.; Landi, B. J. Advanced germanium nanoparticle composite anodes using single wall carbon nanotube conductive additives. *J. Mater. Chem. A* **2014**, *2*, 14528−14535.

(7) Son, I. H.; Hwan Park, J.; Kwon, S.; Park, S.; Rümmeli, M. H.; Bachmatiuk, A.; Song, H. J.; Ku, J.; Choi, J. W.; Choi, J.-m.; Doo, S.-G.; Chang, H. Silicon carbide-free graphene growth on silicon for lithium-ion battery with high volumetric energy density. *Nat. Commun.* **2015**, *6*, 7393.

(8) Lin, D.; Lu, Z.; Hsu, P.-C.; Lee, H. R.; Liu, N.; Zhao, J.; Wang, H.; Liu, C.; Cui, Y. A high tap density secondary silicon particle anode fabricated by scalable mechanical pressing for lithium-ion batteries. *Energy Environ. Sci.* **2015**, *8*, 2371−2376.

(9) Ji, L.; Lin, Z.; Alcoutlabi, M.; Zhang, X. Recent developments in nanostructured anode materials for rechargeable lithium-ion batteries. *Energy Environ. Sci.* **2011**, *4*, 2682−2699.

(10) Bogart, T. D.; Chockla, A. M.; Korgel, B. A. High capacity lithium ion battery anodes of silicon and germanium. *Curr. Opin. Chem. Eng.* **2013**, *2*, 286−293.

(11) Nitta, N.; Yushin, G. High-Capacity Anode Materials for Lithium-Ion Batteries: Choice of Elements and Structures for Active Particles. *Particle & Particle Systems Characterization* **2014**, *31*, 317−336.

(12) Sun, Y.; Liu, N.; Cui, Y. Promises and challenges of nanomaterials for lithium-based rechargeable batteries. *Nat. Energy* **2016**, *1*, 16071.

(13) Li, W.; Sun, X.; Yu, Y. Si-, Ge-, Sn-Based Anode Materials for Lithium-Ion Batteries: From Structure Design to Electrochemical Performance. *Small Methods* **2017**, *1*, 1600037.

(14) Liu, N.; Lu, Z.; Zhao, J.; McDowell, M. T.; Lee, H.-W.; Zhao, W.; Cui, Y. A pomegranate-inspired nanoscale design for large-volume-change lithium battery anodes. *Nat. Nanotechnol.* **2014**, *9*, 187−192.

(15) Yuan, F.-W.; Yang, H.-J.; Tuan, H.-Y. Alkanethiol-Passivated Ge Nanowires as High-Performance Anode Materials for Lithium-Ion Batteries: The Role of Chemical Surface Functionalization. *ACS Nano* **2012**, *6*, 9932−9942.

(16) Kennedy, T.; Mullane, E.; Geaney, H.; Osiak, M.; O'Dwyer, C.; Ryan, K. M. High-Performance Germanium Nanowire-Based Lithium-Ion Battery Anodes Extending over 1000 Cycles Through in Situ Formation of a Continuous Porous Network. *Nano Lett.* **2014**, *14*, 716−723.

(17) Ngo, D. T.; Le, H. T. T.; Kim, C.; Lee, J.-Y.; Fisher, J. G.; Kim, I.-D.; Park, C.-J. Mass-scalable synthesis of 3D porous germanium-carbon composite particles as an ultra-high rate anode for lithium ion batteries. *Energy Environ. Sci.* **2015**, *8*, 3577−3588.

(18) Guo, Y.; Zeng, X.; Zhang, Y.; Dai, Z.; Fan, H.; Huang, Y.; Zhang, W.; Zhang, H.; Lu, J.; Huo, F.; Yan, Q. Sn Nanoparticles Encapsulated in 3D Nanoporous Carbon Derived from a Metal−Organic Framework for Anode Material in Lithium-Ion Batteries. *ACS Appl. Mater. Interfaces* **2017**, *9*, 17172−17177.

(19) Liu, Y.; Zhou, G.; Liu, K.; Cui, Y. Design of Complex Nanomaterials for Energy Storage: Past Success and Future Opportunity. *Acc. Chem. Res.* **2017**, *50*, 2895−2905.

(20) Zhou, J.; Liu, X.; Cai, W.; Zhu, Y.; Liang, J.; Zhang, K.; Lan, Y.; Jiang, Z.; Wang, G.; Qian, Y. Wet-Chemical Synthesis of Hollow Red-Phosphorus Nanospheres with Porous Shells as Anodes for High-Performance Lithium-Ion and Sodium-Ion Batteries. *Adv. Mater.* **2017**, *29*, 1700214.

(21) Chang, W.-C.; Tseng, K.-W.; Tuan, H.-Y. Solution Synthesis of Iodine-Doped Red Phosphorus Nanoparticles for Lithium-Ion Battery Anodes. *Nano Lett.* **2017**, *17*, 1240−1247.

(22) Zhang, R.; Du, Y.; Li, D.; Shen, D.; Yang, J.; Guo, Z.; Liu, H. K.; Elzatahry, A. A.; Zhao, D. Highly Reversible and Large Lithium Storage in Mesoporous Si/C Nanocomposite Anodes with Silicon Nanoparticles Embedded in a Carbon Framework. *Adv. Mater.* **2014**, *26*, 6749−6755.

(23) Tian, M.; Wang, W.; Wei, Y.; Yang, R. Stable high areal capacity lithium-ion battery anodes based on three-dimensional Ni−Sn nanowire networks. *J. Power Sources* **2012**, *211*, 46−51.

(24) Chockla, A. M.; Klavetter, K. C.; Mullins, C. B.; Korgel, B. A. Solution-Grown Germanium Nanowire Anodes for Lithium-Ion Batteries. *ACS Appl. Mater. Interfaces* **2012**, *4*, 4658−4664.

(25) Klavetter, K. C.; Wood, S. M.; Lin, Y.-M.; Snider, J. L.; Davy, N. C.; Chockla, A. M.; Romanovicz, D. K.; Korgel, B. A.; Lee, J.-W.; Heller, A.; Mullins, C. B. A high-rate germanium-particle slurry cast Li-ion anode with high Coulombic efficiency and long cycle life. *J. Power Sources* **2013**, *238*, 123−136.

(26) Kim, N.; Chae, S.; Ma, J.; Ko, M.; Cho, J. Fast-charging high-energy lithium-ion batteries via implantation of amorphous silicon nanolayer in edge-plane activated graphite anodes. *Nat. Commun.* **2017**, *8*, 812.

(27) Wu, H.; Zhuo, D.; Kong, D.; Cui, Y. Improving battery safety by early detection of internal shorting with a bifunctional separator. *Nat. Commun.* **2014**, *5*, 5193.

(28) Kazyak, E.; Wood, K. N.; Dasgupta, N. P. Improved Cycle Life and Stability of Lithium Metal Anodes through Ultrathin Atomic

DOI: 10.1021/acssuschemeng.8b02409
ACS Sustainable Chem. Eng. 2019, 7, 156−164

Layer Deposition Surface Treatments. *Chem. Mater.* **2015**, *27*, 6457−6462.
(29) Bieker, G.; Winter, M.; Bieker, P. Electrochemical in situ investigations of SEI and dendrite formation on the lithium metal anode. *Phys. Chem. Chem. Phys.* **2015**, *17*, 8670−8679.
(30) Lin, D.; Liu, Y.; Cui, Y. Reviving the lithium metal anode for high-energy batteries. *Nat. Nanotechnol.* **2017**, *12*, 194.
(31) Zhang, Q.; Chen, H.; Luo, L.; Zhao, B.; Luo, H.; Han, X.; Wang, J.; Wang, C.; Yang, Y.; Zhu, T.; Liu, M. Harnessing the concurrent reaction dynamics in active Si and Ge to achieve high performance lithium-ion batteries. *Energy Environ. Sci.* **2018**, *11*, 669−681.
(32) Wang, J.; Du, N.; Zhang, H.; Yu, J.; Yang, D. Cu−$Si_{1-x}Ge_x$ core−shell nanowire arrays as three-dimensional electrodes for high-rate capability lithium-ion batteries. *J. Power Sources* **2012**, *208*, 434−439.
(33) Cao, F.-F.; Deng, J.-W.; Xin, S.; Ji, H.-X.; Schmidt, O. G.; Wan, L.-J.; Guo, Y.-G. Cu-Si Nanocable Arrays as High-Rate Anode Materials for Lithium-Ion Batteries. *Adv. Mater.* **2011**, *23*, 4415−4420.
(34) Zhang, C.; Chai, F.; Fu, L.; Hu, P.; Pang, S.; Cui, G. Lithium storage in a highly conductive Cu3Ge boosted Ge/graphene aerogel. *J. Mater. Chem. A* **2015**, *3*, 22552−22556.
(35) Li, X.; Gu, M.; Hu, S.; Kennard, R.; Yan, P.; Chen, X.; Wang, C.; Sailor, M. J.; Zhang, J.-G.; Liu, J. Mesoporous silicon sponge as an anti-pulverization structure for high-performance lithium-ion battery anodes. *Nat. Commun.* **2014**, *5*, 4105.
(36) Ryu, J.; Hong, D.; Shin, S.; Choi, W.; Kim, A.; Park, S. Hybridizing germanium anodes with polysaccharide-derived nitrogen-doped carbon for high volumetric capacity of Li-ion batteries. *J. Mater. Chem. A* **2017**, *5*, 15828−15837.
(37) Lee, G.-H.; Shim, H.-W.; Kim, D.-W. Superior long-life and high-rate Ge nanoarrays anchored on Cu/C nanowire frameworks for Li-ion battery electrodes. *Nano Energy* **2015**, *13*, 218−225.
(38) Liu, Y.; Huang, K.; Fan, Y.; Zhang, Q.; Sun, F.; Gao, T.; Yang, L.; Zhong, J. Three-dimensional network current collectors supported Si nanowires for lithium-ion battery applications. *Electrochim. Acta* **2013**, *88*, 766−771.
(39) Leveau, L.; Laïk, B.; Pereira-Ramos, J.-P.; Gohier, A.; Tran-Van, P.; Cojocaru, C.-S. Silicon nano-trees as high areal capacity anodes for lithium-ion batteries. *J. Power Sources* **2016**, *316*, 1−7.
(40) Lu, Z.; Liu, N.; Lee, H.-W.; Zhao, J.; Li, W.; Li, Y.; Cui, Y. Nonfilling Carbon Coating of Porous Silicon Micrometer-Sized Particles for High-Performance Lithium Battery Anodes. *ACS Nano* **2015**, *9*, 2540−2547.
(41) Li, Y.; Yan, K.; Lee, H.-W.; Lu, Z.; Liu, N.; Cui, Y. Growth of conformal graphene cages on micrometre-sized silicon particles as stable battery anodes. *Nat. Energy* **2016**, *1*, 15029.
(42) Wang, L.; Liu, T.; Peng, X.; Zeng, W.; Jin, Z.; Tian, W.; Gao, B.; Zhou, Y.; Chu, P. K.; Huo, K. Highly Stretchable Conductive Glue for High-Performance Silicon Anodes in Advanced Lithium-Ion Batteries. *Adv. Funct. Mater.* **2018**, *28*, 1704858.
(43) Park, H.; Choi, S.; Lee, S.-J.; Cho, Y.-G.; Hwang, G.; Song, H.-K.; Choi, N.-S.; Park, S. Design of an ultra-durable silicon-based battery anode material with exceptional high-temperature cycling stability. *Nano Energy* **2016**, *26*, 192−199.
(44) Jaumann, T.; Gerwig, M.; Balach, J.; Oswald, S.; Brendler, E.; Hauser, R.; Kieback, B.; Eckert, J.; Giebeler, L.; Kroke, E. Dichlorosilane-derived nano-silicon inside hollow carbon spheres as a high-performance anode for Li-ion batteries. *J. Mater. Chem. A* **2017**, *5*, 9262−9271.
(45) Mo, R.; Rooney, D.; Sun, K.; Yang, H. Y. 3D nitrogen-doped graphene foam with encapsulated germanium/nitrogen-doped graphene yolk-shell nanoarchitecture for high-performance flexible Li-ion battery. *Nat. Commun.* **2017**, *8*, 13949.
(46) Ma, X.; Zhou, Y.; Chen, M.; Wu, L. Synthesis of Olive-Like Nitrogen−Doped Carbon with Embedded Ge Nanoparticles for Ultrahigh Stable Lithium Battery Anodes. *Small* **2017**, *13*, 1700403.
(47) Liang, J.; Li, X.; Hou, Z.; Zhang, T.; Zhu, Y.; Yan, X.; Qian, Y. Honeycomb-like Macro-Germanium as High-Capacity Anodes for Lithium-Ion Batteries with Good Cycling and Rate Performance. *Chem. Mater.* **2015**, *27*, 4156−4164.
(48) Liu, L.; Lyu, J.; Li, T.; Zhao, T. Well-constructed silicon-based materials as high-performance lithium-ion battery anodes. *Nanoscale* **2016**, *8*, 701−722.

DOI: 10.1021/acssuschemeng.8b02409
ACS Sustainable Chem. Eng. 2019, 7, 156−164